

Research Article

EGFET pH Sensor Performance Dependence on Sputtered TiO₂ Sensing Membrane Deposition Temperature

Khairul Aimi Yusof,¹ Rohanieza Abdul Rahman,¹ Muhammad AlHadi Zulkefle,¹
Sukreen Hana Herman,² and Wan Fazlida Hanim Abdullah³

¹NANO-Electronic Centre (NET), Faculty of Electrical Engineering, Universiti Teknologi MARA, 40450 Shah Alam, Selangor, Malaysia

²Core of Frontier Materials & Industry Applications, Faculty of Electrical Engineering, Universiti Teknologi MARA, 40450 Shah Alam, Selangor, Malaysia

³Faculty of Electrical Engineering, Universiti Teknologi MARA, 40450 Shah Alam, Selangor, Malaysia

Correspondence should be addressed to Khairul Aimi Yusof; khairul.aimi.yusof@gmail.com

Received 27 April 2016; Accepted 11 July 2016

Academic Editor: Sang Sub Kim

Copyright © 2016 Khairul Aimi Yusof et al. This is an open access article distributed under the Creative Commons Attribution License, which permits unrestricted use, distribution, and reproduction in any medium, provided the original work is properly cited.

Titanium dioxide (TiO₂) thin films were sputtered by radio frequency (RF) magnetron sputtering method and have been employed as the sensing membrane of an extended gate field effect transistor (EGFET) for pH sensing detection application. The TiO₂ thin films were deposited onto indium tin oxide (ITO) coated glass substrates at room temperature and 200°C, respectively. The effect of deposition temperature on thin film properties and pH detection application was analyzed. The TiO₂ samples used as the sensing membrane for EGFET pH-sensor and the current-voltage (*I-V*), hysteresis, and drift characteristics were examined. The sensitivity of TiO₂ EGFET sensing membrane was obtained from the transfer characteristic (*I-V*) curves for different substrate heating temperatures. TiO₂ thin film sputtered at room temperature achieved higher sensitivity of 59.89 mV/pH compared to the one deposited at 200°C indicating lower sensitivity of 37.60 mV/pH. Moreover the hysteresis and the drift of TiO₂ thin film deposited at room temperature showed lower values compared to the one at 200°C. We have also tested the effect of operating temperature on the performance of the EGFET pH-sensing and found that the temperature effect was very minimal.

1. Introduction

TiO₂ is a type of metal oxide material that has become an important engineering material due to the versatility of electrical and optical properties that have been used in various applications in many fields including dye-sensitized solar cell [1, 2], photocatalysts [3], working electrodes in semiconductor [4], dielectric layers material [5, 6], gas sensor [7], drug sensor [8], and also sensing membrane for pH detection [9–12]. TiO₂ is an interesting material due to its advantages such as good chemical and temperature stability, high permittivity and refractivity index, high dielectric constant, and biocompatibility.

TiO₂ has been widely used as a pH sensor in order to detect H⁺ ions. There are two types of electrochemical sensor that typically have been studied for pH sensing which are ion sensitive field effect transistor (ISFET) [9] and extended

gate field effect transistor (EGFET) [10, 13]. The distinction between these two devices is that ISFET consists of field effect transistor (FET) with sensing membrane that was fabricated together with FET and in contact directly with the electrolyte, while EGFET consists of FET and sensing membrane that are separated into two parts and only the sensing membrane is in contact directly with the electrolyte while the FET is being isolated. EGFET configuration gives more advantages compared to ISFET like low cost, less sensitivity to light and temperature, and also simple packaging [14].

In this work, we report the application of TiO₂ as the sensing membrane of an EGFET pH sensor and its dependence on the deposition temperature are discussed. The deposition temperatures are kept at low range due to the possibility of employing the process for flexible substrates in the future. Then, the physical properties of deposited thin films were examined and also the EGFET sensors were characterized

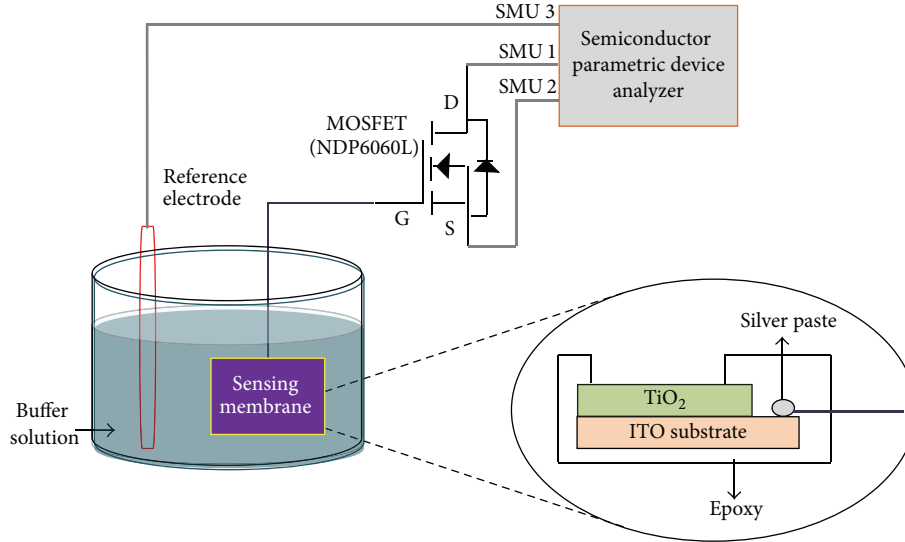


FIGURE 1: EGFET sensor measurement setup.

TABLE 1: RF magnetron sputtering conditions of TiO_2 thin films.

Parameters	Conditions 1	Conditions 2
Substrate heating temperature ($^{\circ}\text{C}$)	Room temperature	200
RF power (W)	300	300
Working pressure (mTorr)	5	5
Gas flow rate (Ar : O_2 sccm)	50 : 1	50 : 1
Deposition time (min)	5	5

for their transfer characteristics, hysteresis, drift, and temperature compensation test. Comparison between EGFET and ISFET was also simulated experimentally to prove the operating temperature stability of EGFET.

2. Methodology

2.1. Fabrication of TiO_2 Sensing Membrane. The TiO_2 sensing membrane was deposited on ITO coated glass that acts as the substrate. At the same time, the conductive layer of ITO was used to be connected to the gate of commercial transistor (NDP6060L). Prior to the deposition process taking place, ITO coated glass was cleaned in an ultrasonic bath for 10 min at 50°C using methanol and deionized water (DIW) alternately to assure the ITO is free from dirt and contamination. Afterward, ITO was dried by nitrogen gas before being ready to be used. Before the deposition process, the target was undergoing presputtered process for about 300 sec to eliminate any contamination on the target surface and stabilize the sputtering conditions. TiO_2 thin films were then deposited on top of cleaned ITO coated glass by RF magnetron sputtering system (SNTEK RSP 5004). The TiO_2 target had high purity of 99.99% and a diameter of 4 inches. The details of RF magnetron sputtering conditions for TiO_2 thin films are summarized in Table 1. The field emission

scanning electron microscope, FESEM (JEOL-JSM 7600F), and Raman spectroscopy (Jobin Yvon Horiba) were used to analyze the surface morphology and structural properties of thin films. Meanwhile, the element composition of TiO_2 was observed by energy dispersive X-ray spectroscopy (EDX) and the surface roughness of TiO_2 was analyzed by using atomic force microscopy (AFM).

2.2. EGFET Sensor: Measurement Setup

2.2.1. Transfer Characteristic (I - V) Measurement Setup. The deposited thin films were prepared for current-voltage (I - V) measurement. Before I - V measurements were carried out, the undeposited area of ITO was connected with metal wire and attached with silver paste. In order to avoid leakage current, the thin films were encapsulated with epoxy resin with $1\text{ cm} \times 1\text{ cm}$ of opening sensing area being defined at the deposited thin film. The completed sensing membrane was then connected to the gate of the commercial MOSFET (NDP 6060L). Then, the encapsulated thin film and reference electrode (Ag/AgCl) were immersed together in various pH buffer solutions of pH of 1.8, 4, 6.2, 7, 8.1, 10, and 12. As reported by [15], reference electrode is needed for proper operation of ISFET so that the electrolyte potential can be established with respect to the semiconductor substrate. By using Semiconductor Parametric Device Analyzer model BI500A, the transfer characteristics and drain current versus reference voltage (I_D - V_{REF}) were obtained. In order to avoid light and environment effect, all measurements were performed in a dark box at room ambient. Figure 1 shows the current-voltage (I - V) measurement setup for EGFET using TiO_2 sputtered sensing membrane.

2.2.2. Hysteresis and Drift Measurement Setting. The measurement system of hysteresis and drift consists of EGFET TiO_2 sensing membrane, reference electrode, constant

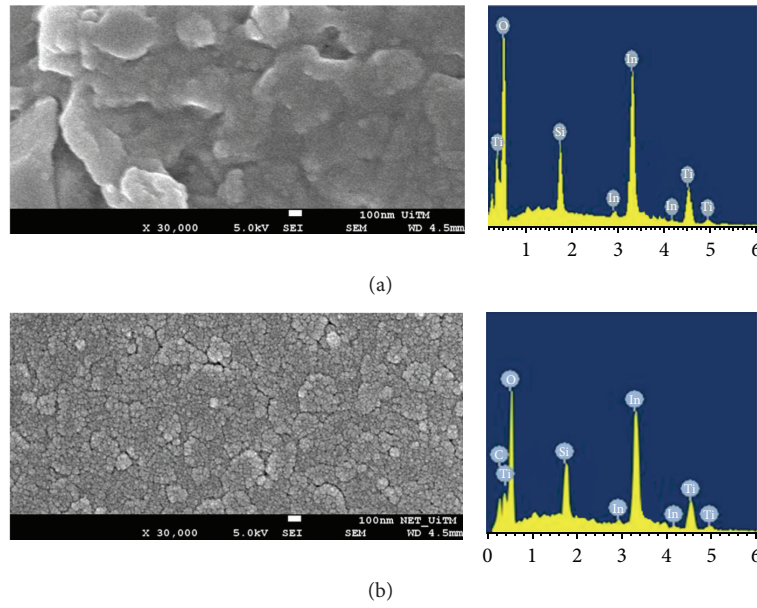


FIGURE 2: Surface morphology and EDX analysis of TiO_2 thin films deposited at (a) room temperature and (b) 200°C .

current constant voltage readout interfacing circuit (CVCC ROIC), data logger, and also a PC with signal recording software. For drift measurement, the deposited TiO_2 sensing membrane and reference electrode were immersed in buffer solution of pH 4 for 12 hours and the output voltage of the TiO_2 sensing membrane was recorded and stored by using a data logger. Meanwhile, a PC is used to display the graph of recording data. The measurement was repeated for various buffer solution of pH of 7, 10, and 12 for 12 hours, correspondingly. Afterward, using the same measurement setting of drift, the hysteresis curves were performed at pH loop of $7 \rightarrow 4 \rightarrow 7 \rightarrow 10 \rightarrow 7$ and $7 \rightarrow 10 \rightarrow 7 \rightarrow 4 \rightarrow 7$ for 500 sec.

2.2.3. EGFET and ISFET Comparison of Temperature Experimental Simulation. This experiment serves as the simulation to experiment the effect of operating temperature on the EGFET and ISFET sensor performance. As mentioned, for ISFET, since the sensing membrane is fabricated directly on the gate of the FET, the transistor will be immersed in the solution during measurement; thus the reading will be influenced by the temperature. On the other hand, for EGFET, only the sensing membrane which acts as the extended gate of the FET will be immersed during the measurement. In this work, we simulated ISFET, by immersing the sensing membrane and MOSFET with reference electrode in pH buffer solutions on top of the hot plate. The temperature of pH buffer solution varied from 24 to 70°C by increasing of 5°C per step. As for EGFET simulation, only the sensing membrane (extended gate) with MOSFET was immersed in pH buffer solutions on top of the hot plate for measurement and the temperature was varied in the same range. The measurement setup consisted of EGFET sensing membrane and reference electrode, commercial MOSFET, constant current constant

voltage readout interfacing circuit (CVCC ROIC), digital multimeter, and a hot plate.

3. Result and Discussion

3.1. Physical Characteristics of the TiO_2 Thin Films. Figures 2(a) and 2(b) show the surface morphologies of the TiO_2 thin films deposited at room temperature and at 200°C , respectively. The images show that different deposition temperature results in different surface structure of thin films. Thin film deposited at room temperature shows a rough and nonuniform surface with mostly undistinguishable grain boundaries. On the other hand, the one at 200°C exhibits small grains and also shows the agglomeration of particles which has a more uniform surface structure. It might have happened due to the higher kinetic energy from the higher temperature of 200°C to restructure TiO_2 particles. The material components of deposited TiO_2 were confirmed by EDX characterization. The EDX shows that both deposited thin films contain titanium (Ti) and oxygen (O_2) elements. Other elements that exist in the thin films like silicon (Si) and indium (In) were from the ITO glass substrate and the carbon (C) peak may originate from the environment contamination. The TiO_2 thin film thickness measured by surface profiler for the thin film deposited at room temperature is 61.55 nm which is slightly thicker compared to that at 200°C which is 60 nm. It can be said that higher temperature induces more agglomeration and a denser film with regard to the film thickness direction resulting in a thinner and compact film. The surface roughness of deposited TiO_2 thin films was analyzed by using atomic force microscopy (AFM), as shown in Figures 3(a) and 3(b). As the substrate temperature increased, the surface roughness of deposited thin films is decreasing. The roughness decreases from 7.123 nm to 2.841 nm as

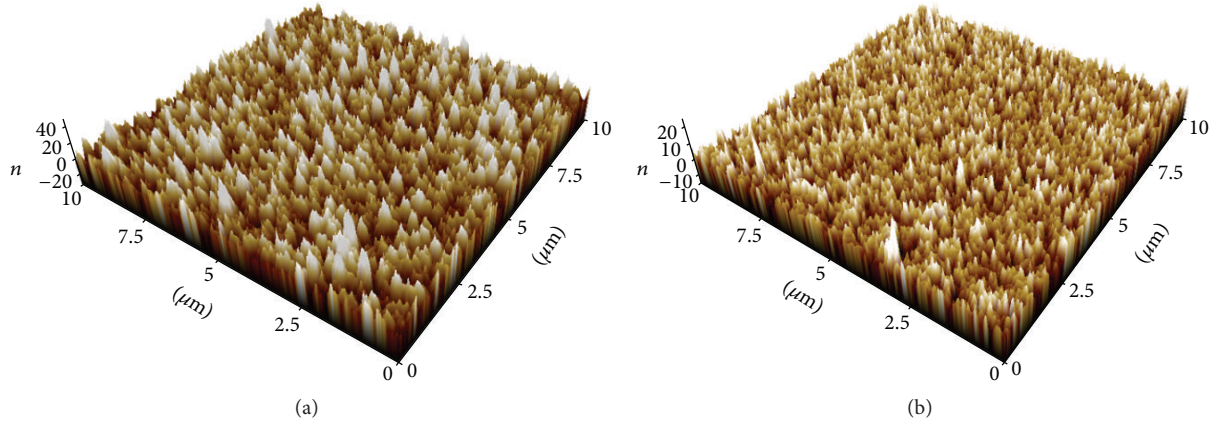


FIGURE 3: AFM images of TiO_2 thin films deposited at (a) room temperature and (b) 200°C .

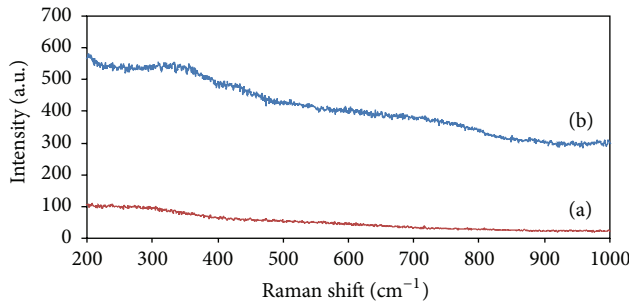


FIGURE 4: Raman spectrum of TiO_2 thin films deposited at (a) room temperature and (b) 200°C .

the substrate temperature increased from room temperature to 200°C , respectively. Via the site-binding model theory, the sensing performance would improve as the number of surface sites increased. The increasing size of grain could improve the properties of sensing performance when the deposited thin film was used as sensing membrane [16]. Figure 4 shows the Raman spectrum of the TiO_2 thin films deposited at room temperature and at 200°C . The measurement was carried out at an excitation wavelength of 514.5 nm in the range of $200\text{--}1000\text{ cm}^{-1}$. Crystalline TiO_2 known as anatase, rutile, and brookite will exhibit Raman shift peaks at 144 , 447 , and 153 cm^{-1} [17–19]. However, from Figure 4, no sharp peak can be observed, which clearly indicates that both deposited TiO_2 thin films have an amorphous structure.

3.2. EGFET Sensor Characterizations

3.2.1. Transfer Characteristics ($I_D\text{--}V_{\text{REF}}$) and pH Sensitivity. Figures 5(a) and 5(b) show the transfer characteristics ($I_D\text{--}V_{\text{REF}}$) of the sputtered TiO_2 thin films in various buffer solutions of pH values between 1.8 and 12. Meanwhile, the corresponding V_{REF} versus pH plot is shown in the inset. The sensitivity and linearity of the sensor were derived from the slope and the linear regression of the graph, respectively. In this measurement, the drain voltage (V_D) was fixed at 500 mV while the reference voltage (V_{REF}) was swept from

-2 to 3 V . Both graphs show similar behaviour of transfer characteristics in which the threshold voltage shifts from left to the right. The shift of the threshold voltage to the right with increasing the pH value is due to the decreasing of the surface potential. The relation of surface potential voltage between sensing membrane and pH buffer solutions can be explained via the site-binding model theory [15]. Figure 6 shows the reactions that occur between the surface of sensing membrane and pH buffer solution. As can be seen from Figure 6, the surface of sensing membrane denoted as Ti can be in three different forms which are negative (TiO^-), positive (TiOH_2^+), and neutral (TiOH). The changes of the surface potential depend on the value of pH buffer solution. The dependence of surface potential voltage (Ψ) between sensing membrane and pH buffer solution can be expressed as [20]

$$2.303 (\text{pH}_{\text{pzc}} - \text{pH}) = \frac{q\Psi}{kT} + \sinh^{-1} \left(\frac{q\Psi}{kT} \cdot \frac{1}{\beta} \right), \quad (1)$$

where pH_{pzc} indicates the pH buffer solution value at the zero charge point, q is the electron charge, k is Boltzmann's constant, T is the absolute temperature, and β is the sensitivity parameter. The relationship of β and the surface sites per unit area could be expressed as [20]

$$\beta = \frac{2q^2 N_s (K_a K_b)^{1/2}}{kT C_{\text{DL}}}, \quad (2)$$

where K_a and K_b are acid equilibrium constant and basic equilibrium constant, respectively, and C_{DL} is the capacitance of the electrical double layer derived by the Gouy-Chapman-Stern model [21]. According to (1), higher linear response of surface potential voltage between sensing membrane and pH buffer solution could be obtained, thus resulting higher sensitivity parameter, β . Therefore, when V_D was fixed, V_G that applied to the commercial MOSFET (NDP 6060L) change with pH buffer solution values.

The sensitivity and linearity for both deposited TiO_2 thin films of different substrate heating temperature are summarized in Table 2. The sensitivity and linearity of deposited TiO_2 thin films were calculated from the output

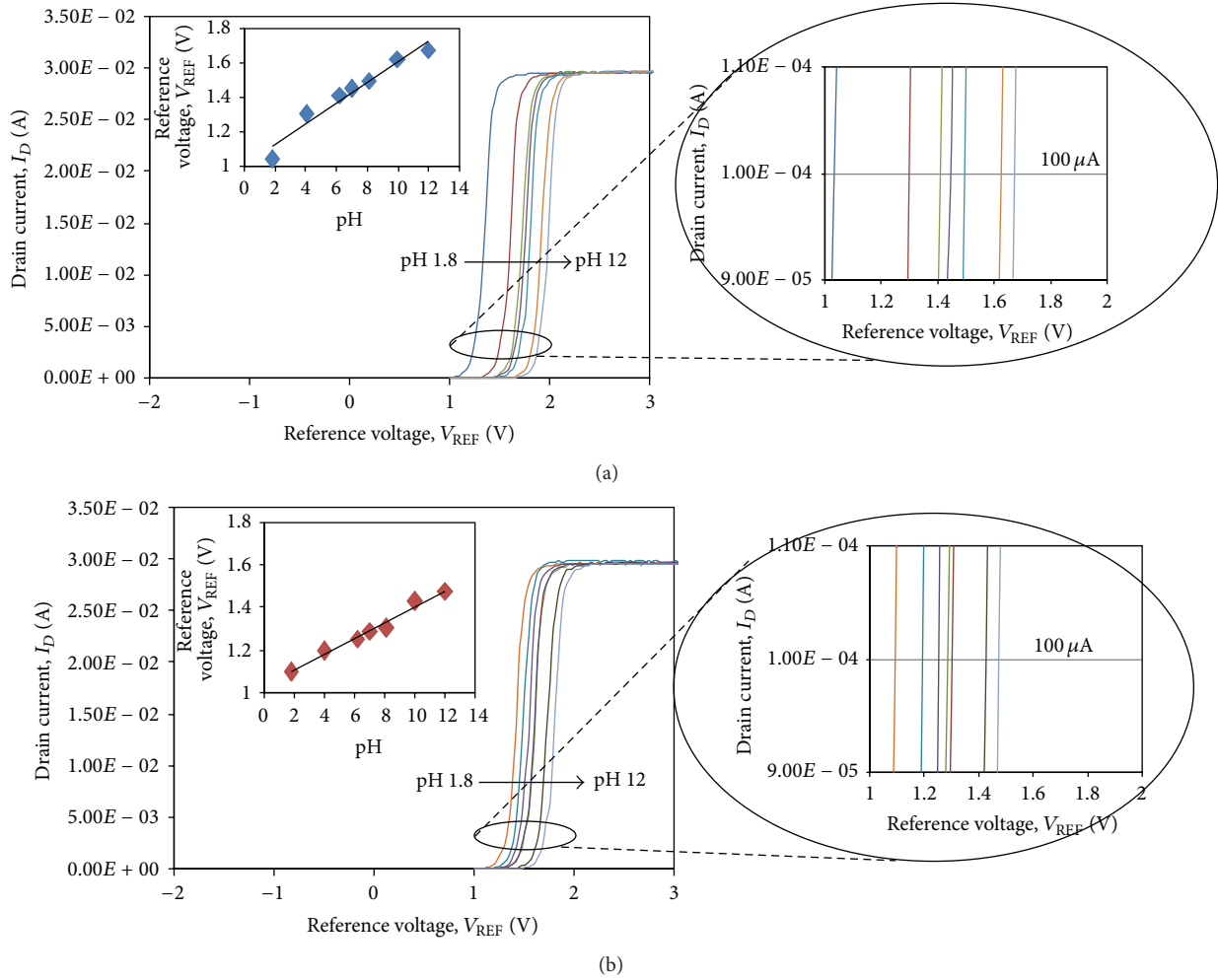


FIGURE 5: Transfer characteristics (I_D - V_{REF}) curve of TiO_2 thin films deposited at (a) room-temperature and (b) $200^\circ C$ at pH of 1.8, 4, 6.2, 7, 8.1, 10, and 12. The inset shows the pH dependence of the reference voltage (V_{REF}) plot. Sensitivity and linearity of the sensor were calculated from this plot.

TABLE 2: Sensitivity and linearity of TiO_2 thin films.

Deposition temperature ($^\circ C$)	Sensitivity (mV/pH)	Linearity
Room temperature	59.89	0.93503
200	37.60	0.95132

voltage taken from the corresponding point at $I_D = 100 \mu A$. The room temperature deposited thin film shows sensitivity and linearity of 59.89 mV/pH and 0.93503, respectively. On the other hand, the sensitivity and linearity obtained by thin film at $200^\circ C$ are 37.60 mV/pH and 0.95132. It is clear that the room temperature TiO_2 thin film shows higher sensitivity and good linearity compared to that of $200^\circ C$. This result could be attributed to the higher surface roughness of TiO_2 thin film deposited at room temperature compared to the one deposited at $200^\circ C$ as observed in the previous surface morphology images (Figure 2) and also from AFM roughness analysis (Figure 3). As reported by many [21–24], higher surface roughness gives better pH sensitivity. Although both thin

films are amorphous as observed by Raman spectroscopy, it can be expected that the thin film deposited at room temperature has a lower degree of crystallinity compared to the sample deposited at $200^\circ C$ which may facilitate more binding sites that relates to higher sensitivity [25]. By comparing to [26], Kao et al. used higher temperature of $800^\circ C$ to obtain higher sensitivity. Meanwhile in this paper, we used lower temperature to produce higher sensitivity yet low cost.

3.2.2. Hysteresis and Drift Characteristics. A hysteresis characteristic of the sensor was measured for output offset voltage corresponding to the change in pH buffer solutions for specified time interval. The sensing membranes were dipped in the pH buffer solutions starting from pH loops of $7 \rightarrow 4 \rightarrow 7 \rightarrow 10 \rightarrow 7$ and $7 \rightarrow 10 \rightarrow 7 \rightarrow 4 \rightarrow 7$ for 500 sec in each pH value. Figures 7(a) and 7(b) show the typical hysteresis loops (V_{OUT} -time) and the hysteresis widths (V_{OUT} -pH) are shown in Figures 7(c) and 7(d). As indicated in Figures 7(c) and 7(d), it is found that TiO_2 thin films deposited at room temperature exhibit a lower output voltage compared

TABLE 3: Output tolerance voltage of TiO₂ thin films deposited at room temperature and 200°C toward pH variations between pH 4 and pH 12 for EGFET and ISFET temperature experimental simulation.

pH	EGFET		ISFET	
	Room temperature (mV/°C)	200°C (mV/°C)	Room temperature (mV/°C)	200°C (mV/°C)
4	0.12043	0.35536	1.7642	1.9817
7	0.29524	0.35754	1.5881	1.8976
10	0.10839	0.35838	1.5973	1.9473
12	0.24868	0.49907	1.5808	1.7671

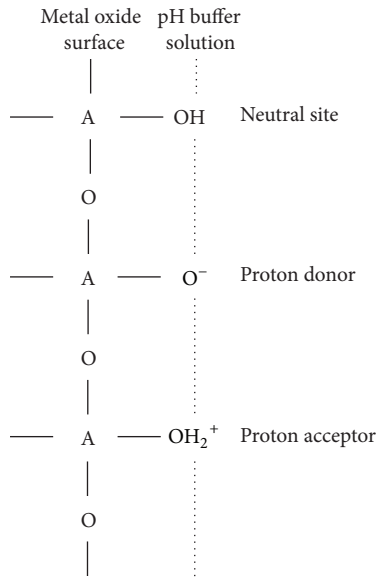


FIGURE 6: Schematic diagram of site-binding model.

to 200°C thin film. This is because of the higher surface roughness of TiO₂ thin films deposited at room temperature, causing the reduction of memory effect [27]. Figure 7(c) demonstrates that the hysteresis width of TiO₂ thin films deposited at room temperature is 5.3 mV and 9 mV in the pH 7 → 4 → 7 → 10 → 7 and 7 → 10 → 7 → 4 → 7 loops, respectively. Meanwhile, the hysteresis width for the one at 200°C is 7.9 mV and 13.8 mV in the same pH loops as shown in Figure 7(d). It is clearly seen that the acid-side hysteresis is smaller than the base-side hysteresis. According to Yao et al., the unsymmetrical hysteresis of pH sensor is due to the difference in the diffusion rates for H⁺ and OH⁻ ions into the buried sites of the sensing membrane [10]. The low hysteresis value indicates good characteristics of electrochemical sensor. This is because high value of hysteresis and drift will limit the accuracy obtained from the sensor [15]. The phenomena of drift and hysteresis could be attributed to the slow progressive hydration of the insulator film as well as to the transport of certain species throughout the insulator film, which affects the semiconductor-insulator interface [15].

The durability and reliability of electrochemical sensor were tested by using drift measurement. The drift measurement was completed in 300 Sec for each pH buffer solution.

The drift characteristics of the TiO₂ thin films measured for pH values of 4–12 plotted as output voltage over time are shown in Figures 8(a) and 8(b). The drift rates of room temperature sample in Figure 8(a) are 0.09766 mV/h, 2.6007 mV/h, 0.59152 mV/h, and 0.041692 mV/h for pH of 4, 7, 10, and 12, respectively. And those for the sample deposited at 200°C were 0.81103 mV/h, 4.4062 mV/h, 0.46916 mV/h, and 0.32618 mV/h. The sensing membrane deposited at room temperature has an obviously smaller drift compared to the one deposited at 200°C, thus indicating the good durability and reliability of pH sensor for 12 hours.

3.2.3. ISFET and EGFET Comparison of Temperature Experimental Simulation. Temperature experimental simulation is the analysis of output voltage response of sensing membranes toward the changes of temperature in various buffer solutions of pH values between 4 and 12. As can be seen in Figures 9(a) and 9(b), the EGFET temperature experimental simulation is shown; meanwhile the ISFET temperature experimental simulation was shown in Figures 9(c) and 9(d). It is apparent from these figures that output voltage response for both sensing membranes toward the changes of solution temperature for EGFET is more stable compared to ISFET. The output tolerance for both thin films deposited at room temperature and 200°C for EGFET and ISFET temperature experimental simulation were summarized in Table 3. For EGFET, both thin films gave lower output tolerance voltage per 1°C. In contrast with ISFET, both thin films showed higher output tolerance voltage per 1°C. From these results, it was proved that having an extended gate for the sensing membrane of sensor system can eliminate the temperature effect on the MOSFET because it was shown that the changes of pH buffer solution temperature did not give significant output voltage value toward the sensing membranes. Indirectly, this temperature compensation test illustrates the advantage of EGFET over ISFET. Hence, EGFET shows better temperature tolerance compared to ISFET which is good for sensor performance.

4. Conclusion

In this work, TiO₂ thin films were prepared using RF magnetron sputtering method at different deposition temperatures onto ITO coated glass substrate for sensing membrane of the EGFET pH sensor. The surface morphology of TiO₂ thin film deposited at room temperature showed a rough

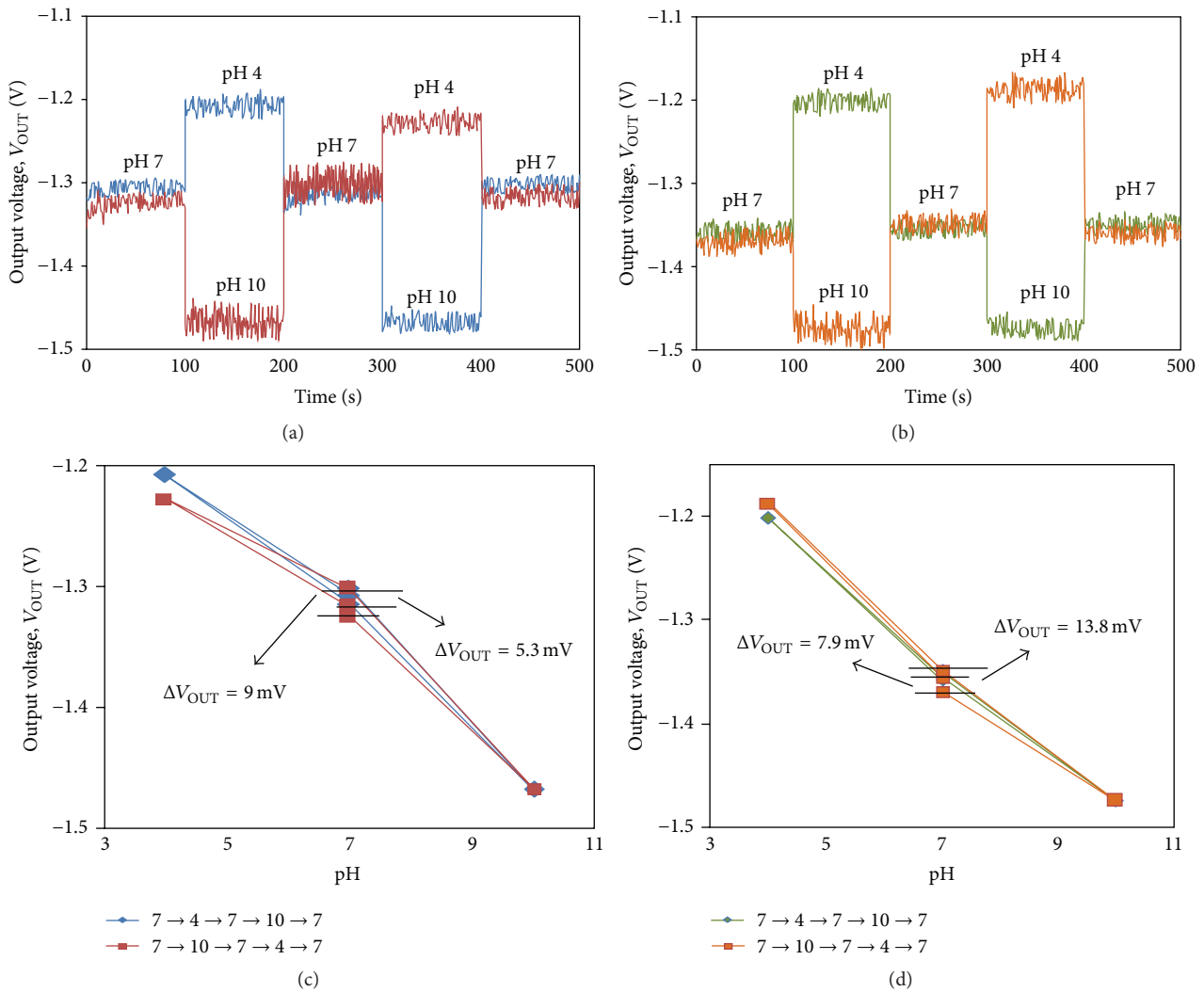


FIGURE 7: Hysteresis characteristics for pH loop of 7 → 4 → 7 → 10 → 7 and 7 → 10 → 7 → 4 → 7 of TiO₂ thin films deposited at (a) room temperature and (b) 200°C. The hysteresis widths are shown in (c) and (d) for TiO₂ thin films deposited at room temperature and 200°C, respectively.

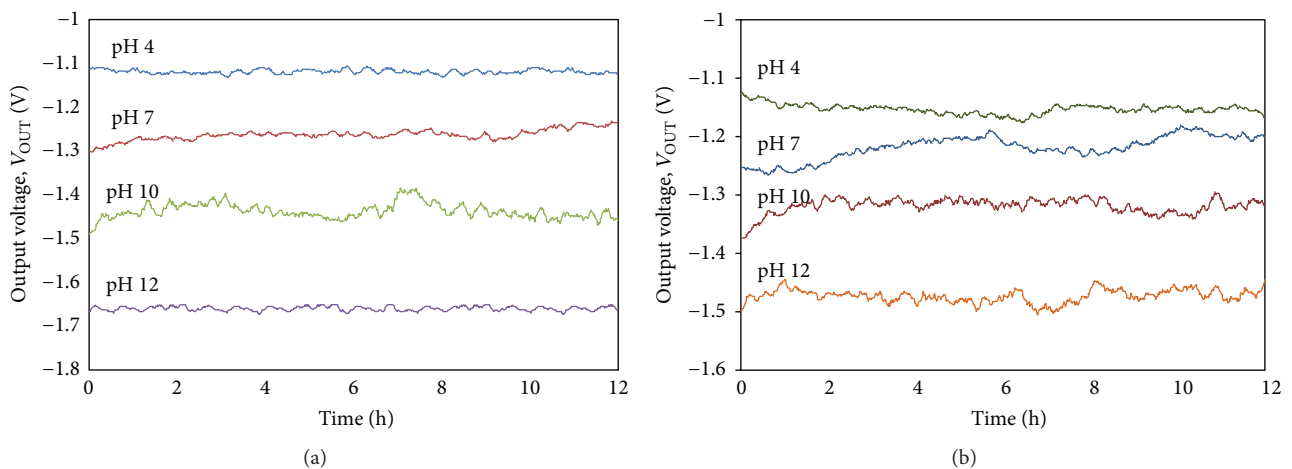


FIGURE 8: Drift characteristics of deposited TiO₂ thin films (a) substrate heating temperature at room temperature and (b) substrate heating temperature at 200°C toward pH variations between pH 4 and pH 12.

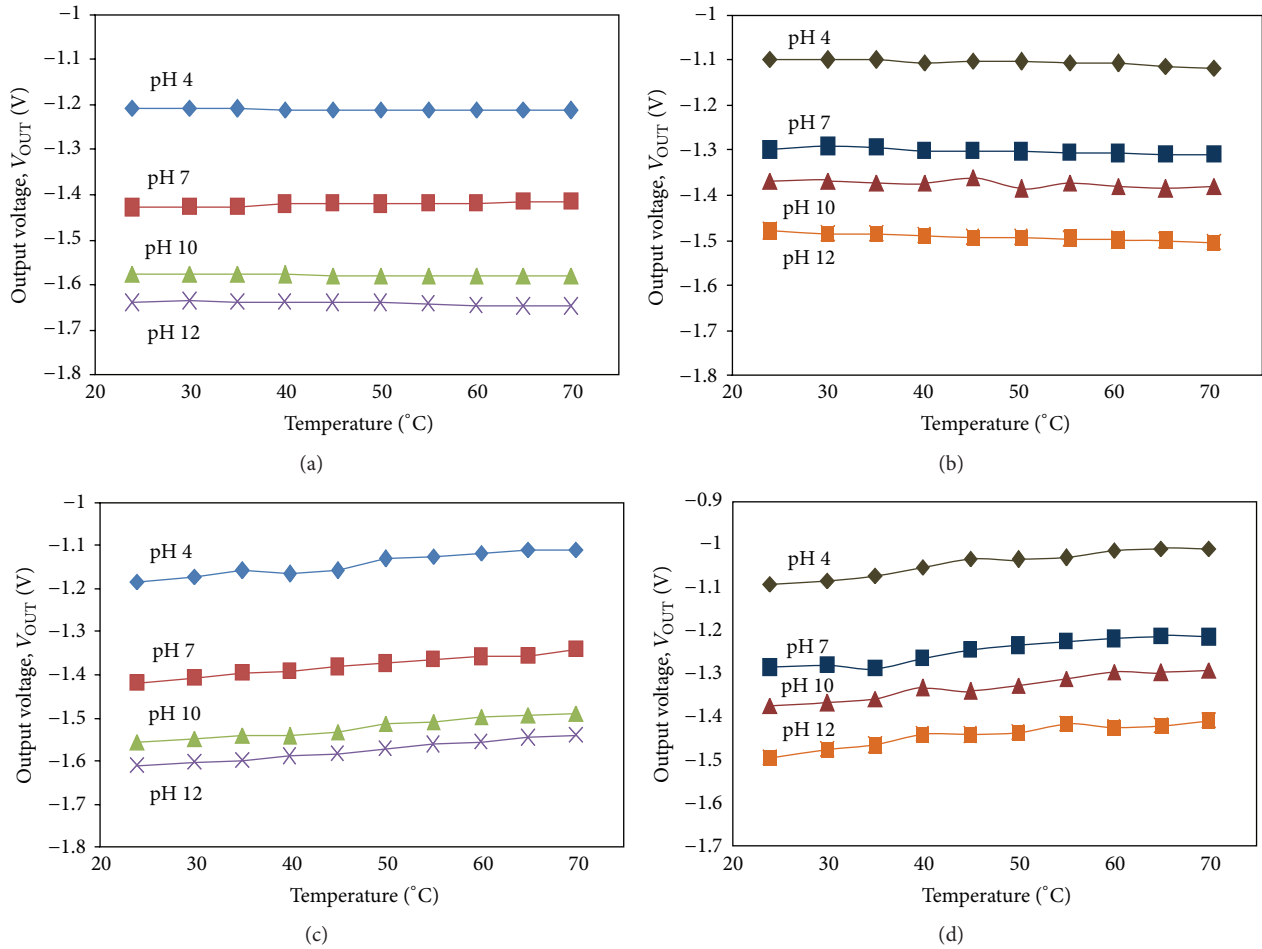


FIGURE 9: EGFET temperature experimental simulation of TiO_2 thin films deposited at (a) room temperature and (b) 200°C and ISFET temperature experimental simulation of TiO_2 thin films deposited at (c) room temperature and (d) 200°C toward pH variations between pH 4 and pH 12.

and nonuniform surface with mostly undistinguishable grain boundaries compared to that of 200°C which exhibits small grains and also shows the agglomeration of particles which has a more uniform surface structure. Typical transfer characteristics ($I_D - V_{\text{REF}}$) for EGFET pH sensor were obtained for each deposited thin film at different temperatures. TiO_2 thin film deposited at room temperature exhibited higher sensitivity and linearity of 59.89 mV/pH and 0.93503 , respectively. In contrast, TiO_2 thin film deposited at 200°C indicated slightly lower sensitivity and linearity of 37.60 mV/pH and 0.95132 , correspondingly. This happened due to the higher surface roughness of TiO_2 thin film deposited at room temperature compared to the one deposited at 200°C as observed in the surface morphology and AFM images. From Raman spectroscopy, both thin films are amorphous; thus it can be expected that the thin film deposited at room temperature has a lower degree of crystallinity compared to the sample deposited at 200°C which may facilitate more binding sites that relates to higher sensitivity. The hysteresis and drift of TiO_2 thin film deposited at room temperature showed lower values compared to the one at 200°C . Low hysteresis and

drift values indicate good characteristics of electrochemical sensor because high value of hysteresis and drift will limit the accuracy of the sensor. The temperature compensation test for both thin films presents likely the same output tolerance voltage; however, it gives a different output tolerance voltage for EGFET and ISFET. EGFET gave lower output tolerance voltage per 1°C compared to ISFET. It can be concluded that TiO_2 thin films deposited at room temperature have good sensitivity, linearity, reliability, and durability which is suitable for pH sensing membrane.

Competing Interests

The authors declare that there are no competing interests regarding the publication of this paper.

Acknowledgments

The authors would like to thank all members of NANO-Electronic Center (NET), Universiti Teknologi MARA, UiTM, and NEMS and Photonics Cluster of MIMOS Berhad

for all the research facilities. The work is partially supported by Ministry of Education Malaysia under the Niche Research Grant Scheme (Project Code 600-RMI/NRGS 5/3(6/2013)).

References

- [1] M. Rani, S. J. Abbas, and S. K. Tripathi, "Influence of annealing temperature and organic dyes as sensitizers on sol-gel derived TiO₂ films," *Materials Science and Engineering: B*, vol. 187, pp. 75–82, 2014.
- [2] M. Ghaffari, M. B. Cosar, H. I. Yavuz, M. Ozenbas, and A. K. Okyay, "Effect of Au nano-particles on TiO₂ nanorod electrode in dye-sensitized solar cells," *Electrochimica Acta*, vol. 76, pp. 446–452, 2012.
- [3] K. Nakata and A. Fujishima, "TiO₂ photocatalysis: design and applications," *Journal of Photochemistry and Photobiology C: Photochemistry Reviews*, vol. 13, no. 3, pp. 169–189, 2012.
- [4] M. Samadpour, S. Giménez, P. P. Boix et al., "Effect of nanostructured electrode architecture and semiconductor deposition strategy on the photovoltaic performance of quantum dot sensitized solar cells," *Electrochimica Acta*, vol. 75, pp. 139–147, 2012.
- [5] L. Yang, J. Qiu, H. Ji, K. Zhu, and J. Wang, "Enhanced dielectric and ferroelectric properties induced by TiO₂@MWCNTs nanoparticles in flexible poly(vinylidene fluoride) composites," *Composites Part A: Applied Science and Manufacturing*, vol. 65, pp. 125–134, 2014.
- [6] S. Kobayashi, K. Amanuma, and H. Hada, "Effect of interconnect layer on Pb(Zr,Ti)O₃ thin film capacitor degradation," *IEEE Electron Device Letters*, vol. 19, no. 11, pp. 417–419, 1998.
- [7] P. X. Zhao, Y. Tang, J. Mao et al., "One-Dimensional MoS₂-Decorated TiO₂ nanotube gas sensors for efficient alcohol sensing," *Journal of Alloys and Compounds*, vol. 674, pp. 252–258, 2016.
- [8] Y.-H. Liao and J.-C. Chou, "Preparation and characterization of the titanium dioxide thin films used for pH electrode and procaine drug sensor by sol-gel method," *Materials Chemistry and Physics*, vol. 114, no. 2-3, pp. 542–548, 2009.
- [9] J.-C. Chou and L. P. Liao, "Study on pH at the point of zero charge of TiO₂ pH ion-sensitive field effect transistor made by the sputtering method," *Thin Solid Films*, vol. 476, no. 1, pp. 157–161, 2005.
- [10] P.-C. Yao, J.-L. Chiang, and M.-C. Lee, "Application of sol-gel TiO₂ film for an extended-gate H⁺ ion-sensitive field-effect transistor," *Solid State Sciences*, vol. 28, pp. 47–54, 2014.
- [11] H. J. N. P. D. Mello and M. Mulato, "Well-established materials in microelectronic devices systems for differential-mode extended-gate field effect transistor chemical sensors," *Microelectronic Engineering*, vol. 160, pp. 73–80, 2016.
- [12] R. A. Rahman, M. A. Zulkefle, W. F. H. Abdullah, and S. H. Herman, "Effect of post deposition annealing process on the pH sensitivity of spin-coated titanium dioxide thin film," *Applied Mechanics and Materials*, vol. 749, pp. 197–201, 2015.
- [13] T. Minami, Y. Sasaki, T. Minamiki et al., "Selective nitrate detection by an enzymatic sensor based on an extended-gate type organic field-effect transistor," *Biosensors and Bioelectronics*, vol. 81, pp. 87–91, 2016.
- [14] E. M. Guerra, G. R. Silva, and M. Mulato, "Extended gate field effect transistor using V₂O₅ xerogel sensing membrane by sol-gel method," *Solid State Sciences*, vol. 11, no. 2, pp. 456–460, 2009.
- [15] C. D. Fung, P. W. Cheung, and W. H. Ko, "A generalized theory of an electrolyte-insulator-semiconductor field-effect transistor," *IEEE Transactions on Electron Devices*, vol. 33, no. 1, pp. 8–18, 1986.
- [16] C.-H. Kao, H. Chen, L.-T. Kuo et al., "Multi-analyte biosensors on a CF₄ plasma treated Nb₂O₅-based membrane with an extended gate field effect transistor structure," *Sensors and Actuators B: Chemical*, vol. 194, pp. 419–426, 2014.
- [17] S. K. Gupta, J. Singh, K. Anbalagan et al., "Synthesis, phase deposition and characterization of rutile nanocrystalline titanium dioxide (TiO₂) thin films," *Applied Surface Science*, vol. 264, pp. 737–742, 2013.
- [18] P. B. Nair, V. B. Justinictor, G. P. Daniel et al., "Structural, optical, photoluminescence and photocatalytic investigations on Fe doped TiO₂ thin films," *Thin Solid Films*, vol. 550, pp. 121–127, 2014.
- [19] N. D. Boscher, S. Olivier, R. Maurau et al., "Photocatalytic anatase titanium dioxide thin films deposition by an atmospheric pressure blown arc discharge," *Applied Surface Science*, vol. 311, pp. 721–728, 2014.
- [20] H.-K. Liao, L.-L. Chi, J.-C. Chou, W.-Y. Chung, T.-P. Sun, and S.-K. Hsiung, "Study on pHpzc and surface potential of tin oxide gate ISFET," *Materials Chemistry and Physics*, vol. 59, no. 1, pp. 6–11, 1999.
- [21] K. B. Oldham, "A Gouy-Chapman-Stern model of the double layer at a (metal)/(ionic liquid) interface," *Journal of Electroanalytical Chemistry*, vol. 613, no. 2, pp. 131–138, 2008.
- [22] T.-M. Pan, J.-C. Lin, M.-H. Wu, and C.-S. Lai, "Structural properties and sensing performance of high-k Nd₂TiO₅ thin layer-based electrolyte-insulator-semiconductor for pH detection and urea biosensing," *Biosensors and Bioelectronics*, vol. 24, no. 9, pp. 2864–2870, 2009.
- [23] M.-H. Wu, C.-H. Cheng, C.-S. Lai, and T.-M. Pan, "Structural properties and sensing performance of high-k Sm₂O₃ membrane-based electrolyte-insulator-semiconductor for pH and urea detection," *Sensors and Actuators B: Chemical*, vol. 138, no. 1, pp. 221–227, 2009.
- [24] T.-M. Pan, K.-Y. Chang, C.-W. Lin, S.-W. Tsai, and M.-H. Wu, "Label-free detection of uric acid using a disposable poly-N-isopropylacrylamide as an encapsulating enzyme material based on high-κ Eu₂Ti₂O₇ electrolyte-insulator-semiconductor devices," *Sensors and Actuators, B: Chemical*, vol. 160, no. 1, pp. 850–857, 2011.
- [25] P. Bergveld, "ISFET, theory and practice," in *Proceedings of the IEEE Sensor Conference*, pp. 1–26, Toronto, Canada, October 2003.
- [26] C. H. Kao, H. Chen, and C.-Y. Huang, "Effects of Ti addition and annealing on high-k Gd₂O₃ sensing membranes on polycrystalline silicon for extended-gate field-effect transistor applications," *Applied Surface Science*, vol. 286, pp. 328–333, 2013.
- [27] T.-M. Pan and K.-M. Liao, "Comparison of structural and sensing characteristics of Pr₂O₃ and PrTiO₃ sensing membrane for pH-ISFET application," *Sensors and Actuators B: Chemical*, vol. 133, no. 1, pp. 97–104, 2008.



Hindawi

Submit your manuscripts at
<http://www.hindawi.com>

